ISBN: 978-3-95450-214-1 ISSN: 2673-5490 doi:10.18429/JACoW-IPAC2021-TUPAB245

WAKEFIELD AND HEAT LOAD STUDY OF THE GATE VALVES AT ILSF STORAGE RING*

N. Khosravi†, S. Dastan, E. Ahmadi
Institute for Research in Fundamental Sciences (IPM), Tehran, Iran
M. Akhyani, Ecole Polytechnique Fédérale de Lausanne (EPFL), Lausanne, Switzerland
A. Khosravi, Shahid Beheshti University, Laser-Plasma Research Institute (LAPRI), Tehran, Iran

Abstract

As one part of the ILSF storage ring, the rf-shield of the gate valves generates considerable interest in terms of wake impedance and heat-load. Inside the gate valves, there is a vacuity that causes low-frequency resonances, leading to beam instabilities. Therefore, controlling and eliminating these frequencies will be substantial. A radio frequency rf-shield structure, which conceals this transverse gap of the gate valves, is indispensable for low emittance chambers. This paper analyzes the wake impedance and thermal behavior of a finger-band RF shield in the gate valve.

INTRODUCTION

The ILSF storage ring is a third-generation low-emittance synchrotron machine [1, 2], generating considerable interest in collective effects. The wakefield and impedance study of the components is going on at the ILSF beam dynamics group [3].

The ILSF storage ring contains 20 super-periods. Both sides of these sections are equipped with gate-valves to preserve the internal vacuum in all the machine's running steps. There is an empty vacuity at the interior part of the gate valves. The dimensional order of the emptiness is around a centimeter. Some destructive resonance peaks in low frequencies are expected in the empty vacuity of the gate-valves. Therefore, some rf-shields should be added to the gate valves to reduce the beam impedance and suppress beam instabilities.

In the first section of this article, the wakefield study was done based on the CST results. Then the longitudinal impedance results were then applied to the power-loss calculation. Finally, the heat load computation is presented here.

Geometry & CST Design

Several profiles of the finger-band shields were simulated and analyzed for the ILSF vacuum chamber. The optimized model of the finger band is presented in Fig. 1.

The beam traveling inside a complicated vacuum chamber induces electromagnetic fields, which may affect the dynamics of the beam itself. In this situation, an accelerator can be seen as a feedback device. Any longitudinal or transverse perturbation appearing in the beam distribution may be amplified (or damped) by the electromagnetic forces generated by the perturbation itself.

For the project's stable operation, the geometry of the rf-shields should improve to have good thermal strength and low beam instabilities. Therefore, both of these aspects are simulated and analyzed in CST solvers.

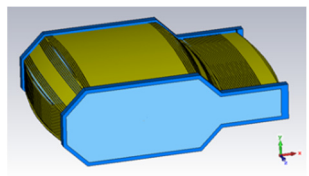

Figure 1: The optimized finger-band RF-Shield for the gate valves.

Simulation Details

CST simulations are evaluated for the 1.6 mm bunch length, normal background, open boundaries in the beam direction, and stainless steel material (LN316).

The wakefield results are prepared for the longitudinal and transverse directions. As it is known, the longitudinal impedance peaks are responsible for heat loss. Also, the transverse impedance peaks are essential in beam instability studies.

In CST simulation, the global mesh setting was not used. Instead, the local mesh setting was added to the critical points of the geometry. The line per sigma was set to 20, and the local mesh properties in z-direction were set to 0.1 mm. Consequently, the number of mesh cells reached 110 million cells.

WAKE FIELD & IMPEDANCES

Wake potentials are calculating in the time domain. A Fast Fourier Transform (FFT) can switch the results to the frequency domain. The longitudinal and transverse results should be studied separately.

Transverse Direction

Figures 2 and 3 contain the transverse results in the Y and X-direction.

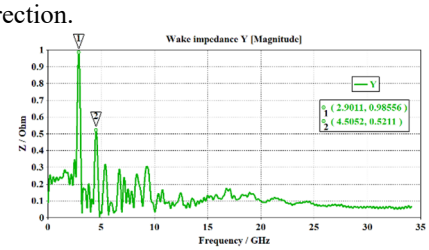

Figure 2: The transverse impedance of the finger-band RF-shield in Y-direction.

* Work supported by Iranian Light Source Facility
† n.khosravi@ipm.ir

ISBN: 978-3-95450-214-1 ISSN: 2673-5490 doi:10.18429/JACoW-IPAC2021-TUPAB245

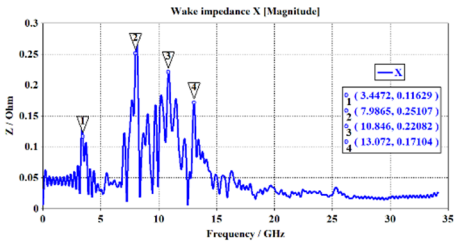

Figure 3: The transverse impedance of the finger-band RF-shield in X-direction.

Based on the transverse impedance results, The Y-direction contains higher instability impedance peaks. one expected an instability study in this direction for this type of RF-shields.

The kick factors are calculated based on a 7.9 mm bunch length. The evaluated amounts are presented in Table 1.

Table 1: The Calculated Kick Factors for a 7.9 mm Bunch-Length

RF-Shield Type	Kick Factor X (K_x) [V/pC/mm]	Kick Factor Y (K_y) [V/pC/mm]
Finger-band	1.68e-3	2.67e-3

Longitudinal Direction

The longitudinal wake potential of the discussed geometry is shown in Fig. 4. There are two resonance peaks at 7.81 and 9.8 GHz which fundamentally responsible for the heat-load effects.

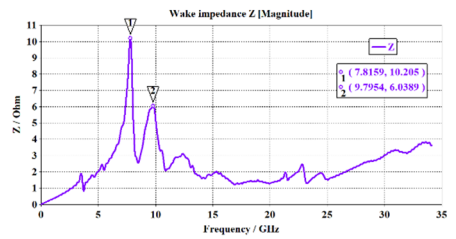

Figure 4: The longitudinal impedance of the finger-band RF shield.

The critical role of thermal stability in vacuum components is clear for all readers. As concluded in previous parts, the finger-band shields are more flexible and less destructive for the beam current. However, the high flexibility of this component makes it sensitive to thermal features. Also, having a cooling system is impossible on the finger-bands. Therefore, it should verify permanently.

POWER LOSS

The most famous equation in power loss calculations is [4]

$$P_{Loss} = -N_{bunch} \frac{q^2}{T_0} K_{Longitudinal} \,. \quad (1)$$

In this equation, the revolution time $T0$ is 1.76 μs. For the peak current 400 mA, and 140 electron bunch, we have q = 5.0286 nC. The evaluated loss factor and power loss are presented in Table 2.

Table 2: Heat Load and Power Loss for a 7.9 mm Bunch Length, 140 Bunch and 40 Gate-Valves at the Storage Ring

The Number of the Gate-Valves	Loss Factor Z (K_z) [V/pC]	Power Loss for 140 bunches (P_L) [KW]
1	1.48e-2	0.029
40	0.592	1.2

HEAT-LOAD

Each resonance peak has its distribution and should be considered separately. By defining an H-monitor in the Wakefield solver of the CST software, these two resonance modes' loss power contribution is calculated individually.

H-Monitors can evaluate the dissipated power into a button by a surface integral [5]

$$P_W = \frac{1}{2}\sqrt{\frac{\pi\mu f}{\sigma}} \int \left|\vec{H}_{\tan}\right|^2 ds \,. \quad (2)$$

The calculation is based on a perturbation method for all solver types. It depends on the frequency f, the specified conductivity σ, and the permeability μ. As mentioned, H is the tangential magnetic field of a loss-free model.

Extending the calculation to the coupled-bunch effect causes an increase in the net beam power experienced by the house part of the BPM. Nagaoka et al. inserted the damping time of the trapped mode in energy loss calculations to include the coupled-bunch effect. Then they integrated the results over time [6].

Here we tried to apply the effect of the quality factor on the coupled-bunch effect to involve the Nagaoka considerations in our simulations.

The quality factor is defined by the stored energy U, transient time factor T, and angular frequency ω.

$$Q = \frac{\omega U}{T} \,. \quad (3)$$

Therefore, the attenuation factor is derived by $\alpha = \frac{\omega}{2Q}$. Then, the electric and magnetic field usually are attenuate with $e^{-\alpha t}$ [7].

One needs an excitation signal based on the real bunches in the storage ring to apply the multi-bunch beam effect in transient thermal solutions. A periodic excitation signal, proportional to our gaussian bunch length and bunch distances were defined. Then it is attached to power loss distribution. Considering the quality factor of the trapped mode, we can apply an attenuation factor to the excitation signal. Figure 5 shows our periodic signal that simulates the bunch length and the bunch distance at the ILSF storage ring. The attenuation factor is approximated to a linear curve.

We can simulate a time-dependent heat load, by repeating the signal in Fig. 5 periodically. It keeps the resonances in the BPM until the attenuation time reach. Now the quality factor of each peak is considered.

ISBN: 978-3-95450-214-1 ISSN: 2673-5490 doi:10.18429/JACoW-IPAC2021-TUPAB245

At last, by switching to the MPHYSICS studio in CST, we can apply the loss power distribution and run the transient thermal solver.

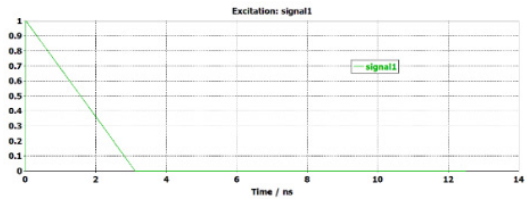

Figure 5: The periodic excitation signal that is applied to power loss distribution.

Extreme caution should be considered on the mesh properties of the component. Applying too precise mesh cells in all components is too time-consuming. Therefore, local mesh properties were used to critical points. It increases the accuracy and decreases the program's running time.

There is one issue that we want to discuss at this point. The imported energy in the CST power loss calculation is proportional to 1.6 mm bunch length. It is not equal to the natural bunch length of the ILSF storage ring (7.9 mm). Although, the resonance distribution of power loss is calculated accurately. Therefore, the power distribution should be preserved, and a rescaling factor should modify the total energy of the loss.

The power loss contribution of each resonance mode is evaluated by Eq. (2). Two resonance peaks at 7.81 and 9.8 GHz are selected from the impedance results. They appended the loss factor integration to calculate the power loss.

As it said, the loss distributions should be normalized to total power loss. Then it multiplies in newly calculated power loss. So, the correction factor for each peak computes. It should be mentioned that all these calculations are done for the power loss of one bunch.

The symmetric thermal boundaries were adjusted for the simulations. The maximum step width in the time integral setting decreased to 0.01 ns, to cover the excitation signal accuracy. The thermal results are prepared and depicted in Figs. 6 and 7.

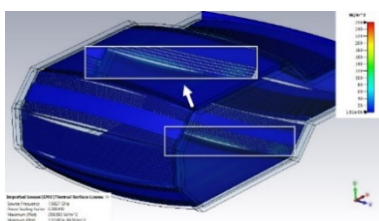

Figure 6: Rescaled power loss distribution at 7.81 GHz.

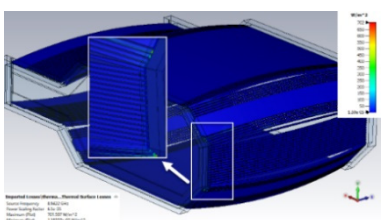

Figure 7: Rescaled power loss distribution at 9.8 GHz.

Also, the direction of heat-flow density toward open boundaries is shown in Fig. 8.

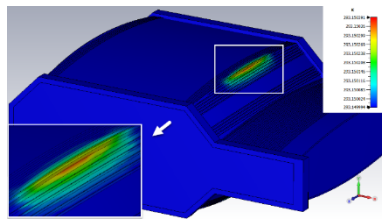

Figure 8: Final Result of thermal heat-load calculations.

As outlined in the thermal literature reviews, by increasing the temperature from $T1$ to $T2$, the relationship between the time elapsed during the temperature variation can be expressed by the following equation:

$$T = (T_2 - T_1)(1 - e^{-\frac{t}{\tau}}) + T_1 . \quad (4)$$

By extracting the maximum temperature in the finger-band geometry and fitting Eq. (4) on it, the thermal behavior of this type of gate valves clear. Figure 9 shows the fitted equation and the extrapolation of the curve.

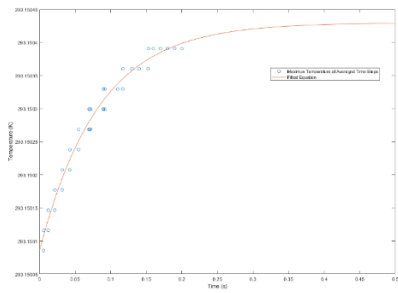

Figure 9: Maximum temperature in averaged time-steps and the extrapolation of the fitted equation.

The utmost caution of finger-band rf shields in all vacuum components should be considered in the thermal characteristics. A thermal study of wakefield effects has been done in the CST MPHYSICS studio. The maximum point of thermal transient solver result's extrapolation clarifies that finger-band geometry can control and damp the extra thermal heat-load on itself.

CONCLUSION

In this paper, the single bunch instabilities are tracked for the finger band-type rf-shield. Considering the result of the wakefield, impedance, and the heat load result posed in our study, it is possible to state that the finger-band type of gate-valves is proper and can be suggested for the ILSF storage ring.

ACKNOWLEDGMENTS

The Iranian Light Source Facility supported this work. Many Thanks to Dr. Hossein Karimi from the vacuum group, and many thanks to Mr. Danaee Fard from the mechanic team for supportive and helpful suggestions.

ISBN: 978-3-95450-214-1 ISSN: 2673-5490 doi:10.18429/JACoW-IPAC2021-TUPAB245

REFERENCES

[1] E. Ahmadi, M. Jafarzadeh, J. Rahighi, H. Ghasem, and S. M. Jazayeri, "Designing an Ultra Low Emittance Lattices for Iranian Light Source Facility Storage Ring", in *Proc. 7th Int. Particle Accelerator Conf. (IPAC'16)*, Busan, Korea, May 2016, pp. 2858-2860. doi:10.18429/JACoW-IPAC2016-WEPOW016

[2] S. Dastan, E. Ahmadi, A. Mash'al, J. Rahighi, and R. Saffari, "MOGA optimization for the ILSF low-beta lattice storage ring", *J. Instrum.*, vol. 15, no. 02, p. P02009, 2020. doi:10.1088/1748-0221/15/02/p02009

[3] N. Khosravi, M. Akhyani, E. Ahmadi, A. Mashal, H. Karimi, and S. Dastan, "A General Comparison on Impedance Theory and CST Simulation of Discontinuities", *J. Phys. Conf. Ser.*, vol. 1350, p. 012122, 2019. doi:10.1088/1742-6596/1350/1/012122

[4] A. W. Chao, *Physics of Collective Beam Instabilities in High Energy Accelerators*. New York, NY, USA: Wiley, 1993.

[5] CST Studio Suite, https://www.cst.com

[6] R. Nagaoka, J. C. Denard, and M. P. Level, "Recent Studies of Geometric and Resistive-wall Impedance at SOLEIL", in *Proc. 10th European Particle Accelerator Conf. (EPAC'06)*, Edinburgh, UK, Jun. 2006, paper THPCH033, pp. 2850-2852.

[7] T. Weiland and R. Wanzenberg, "Wake fields and impedances", in *Frontiers of Particle Beams: Intensity Limitations*, M. Dienes, M. Month, and S. Turner, Eds. Heidelberg, Germany: Springer, 1992, pp. 39-79.